Article

Development and Validation of a Chromatographic Method for Ibrutinib Determination in Human and Porcine Skin

Lucas F. F. Albuquerque [1], Maria Victoria Souto [2], Felipe Saldanha-Araujo [3], Juliana Lott Carvalho [2],
Tais Gratieri [1], Marcilio Cunha-Filho [1] and Guilherme M. Gelfuso [1,*]

1 Laboratory of Food, Drugs, and Cosmetics (LTMAC), School of Health Sciences, University of Brasilia,
  Brasília 70910-900, DF, Brazil
2 School of Medicine, University of Brasilia, Brasília 70910-900, DF, Brazil
3 Laboratory of Hematology and Stem Cells (LHCT), School of Health Sciences, University of Brasilia,
  Brasília 70910-900, DF, Brazil; felipearaujo@unb.br
* Correspondence: gmgelfuso@unb.br

Abstract: Ibrutinib (IBR) is a tyrosine kinase inhibitor investigated for treating solid and non-solid tumors. Considering the advantages that a topical application of IBR could generate in terms of dose reduction and side effects in skin cancer treatment, this paper presents a simple and selective HPLC method for determining IBR concentration in in vitro skin permeation studies to support the development of topical formulations. The method uses a reversed-phase C_{18} column and a mobile phase composed of acetonitrile and 0.01 mol/L phosphoric acid at pH 3.5 (35:65 v/v), flowing at 1.0 mL/min. The oven temperature was set at 35 °C, the injection volume was 20 μL, and UV drug detection was performed at 259 nm. The validation procedure certified that this method was selective for IBR determination even when extracted from human or porcine skin matrices. The method was linear over a range of 0.2 to 15.0 μg/mL, precise, robust, and accurate, with recovery rates from the skin layers higher than $89.5 \pm 5.9\%$ for the porcine skin and higher than $92.0 \pm 0.2\%$ for the human skin. The limits of detection and quantification were 0.01 and 0.02 μg/mL, respectively. The method showed, therefore, to be adequate for use in further skin permeation studies employing IBR topical formulations.

Keywords: bioanalytical method; HPLC; topical formulation

1. Introduction

Ibrutinib (1-[(3R)-3-[4-amino-3-(4-phenoxyphenyl)-1H-pyrazolo[3,4-d]pyrimidin-1-yl]-1-piperidinyl]-2-propen-1-one) is a tyrosine kinase inhibitor investigated for treating both solid and non-solid cancers (Figure 1). The FDA has approved IBR as a monotherapy for treating hematological cancers, including chronic lymphocytic leukemia, mantle cell lymphoma, and macroglobulinemia [1]. The main target of IBR is Bruton's tyrosine kinase (BTK), an enzyme that plays a crucial role in the function of the B-cell receptor (BCR) signaling pathway [1,2]. IBR inhibits BTK through covalently binding to Cys 481, located in the ATP-binding domain [1,2]. Interestingly, this cysteine residue is also present in other tyrosine kinase proteins, which allows IBR to act on additional molecular targets, such as four members of the TFK family (ITK, TEC, BMX, and RLK/TXK), three kinases of the EGFR family (EGFR, ErbB2/HER2, and ErbB4/HER4), and two other kinases, BLK and JAK3 [1–4]. Furthermore, IBR can act on other therapeutic targets, such as the IL-2-inducing kinase (ITK) associated with activating the NF-KB pathway [2,5]. The broad range of targets of IBR have demonstrated its promising effects against several solid tumors [1,2], including breast cancer [1,6], gastric cancer [7], and potentially skin cancers such as melanoma and non-melanoma.
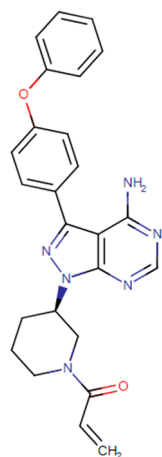
Figure 1. IBR molecular structure.

Although IBR shows excellent promise as a therapeutic agent, its administration presents several challenges. One of the primary issues is related to drug bioavailability. IBR has low aqueous solubility (about 0.002 mg/mL) and is subject to pronounced first-pass metabolism, resulting in an oral bioavailability of only 2.9% [8,9], which can be highly affected by the patient's nutritional status [9–11]. Thus, oral medications are available in high-dose presentations, which can reach up to 840 mg/day depending on the type of cancer being treated, exacerbating the occurrence of side effects [2,3,11], which include atrial fibrillation, bleeding, hypertension, myalgia, anemia, infections, and diarrhea [2,12]. As a result, around 20% of patients may need to discontinue treatment due to severe adverse reactions [13].

Topical administration has emerged as an effective method for delivering some chemotherapeutics for tumors that affect superficial tissues, such as skin cancers, as recently reviewed [14]. This administration route provides several benefits, including reducing or eliminating the side effects associated with oral administration, avoiding drug interactions, and reducing drug doses, which results in a safer and more cost-effective product with ease of administration [15,16].

However, developing new formulations dedicated to topical application requires a reliable analytical method to detect and quantify IBR [15]. Still, quantifying a drug extracted from a complex biological matrix such as the skin is complex [15,17] since many substances extracted from this matrix can interfere with the analysis. Furthermore, even though some methods have been reported for the detection and quantification of IBR, they have been developed explicitly for IBR quantification in the presence of other biological contaminants, such as human or rabbit plasma [8,18]. Also, the only reported method to quantify IBR from skin samples used mouse skin and was not entirely validated [19]. Thus, developing an analytical model that incorporates porcine and human skin would be advantageous, as these models are considered gold standards for cutaneous permeation studies [20].

Therefore, this study aimed to validate a simple chromatographic method for determining the concentration of IBR in porcine and human skin, thereby facilitating the development of topical formulations for cutaneous cancers treatment. Furthermore, this study focuses explicitly on IBR detection in distinct skin layers, as it is crucial to monitor the drug's skin delivery [17], intending to achieve targeted drug delivery to a desired site of action, supporting in vitro studies on skin permeation.

2. Materials and Methods

2.1. Material

IBR standard (>99%) was purchased from Cayman Chemical (Ann Arbor, MI, USA). Acetonitrile and methanol of chromatographic grade and phosphoric acid were purchased from Dinamica (São Paulo, Brazil). Scotch® 845 book tape (3 M, St. Paul, MN, USA) was

used to perform the tape stripping of skin. All analyses were performed with ultrapure water (Millipore, Illkirch-Graffenstaden, Strasbourg, France).

2.2. Obtaining Porcine and Human Skin

Porcine ear skin was obtained from a local slaughterhouse, and human skin fragments were obtained from surgical centers during abdominoplasty procedures (approved by the Ethics Committee of the University of Brasilia, protocol number 30175020.0.0000.5558). In both cases, the material was transported to the laboratory under refrigeration, and the skin was cleaned and separated from adipose tissue, muscle, and blood vessels using scissors. The skin was then cut into circles with an approximate area of 2 cm^2 and stored at -4 °C for 30 days before use.

2.3. Preparation of IBR Stock Solutions

IBR stock solutions were prepared by dissolving 10 mg of the drug in 10 mL methanol to yield a 1 mg/mL concentration. These solutions were stored at 4 °C until further use.

2.4. Tape Stripping

The tape-stripping technique was used to separate the stratum corneum (SC) from the remaining skin (RS). First, the porcine skin fragments were affixed to a foam support with the stratum corneum facing upwards. Next, adhesive tapes were used to remove the stratum corneum, with each tape fixed onto the stratum corneum and then removed with a single motion, repeating the process 15 times for each skin fragment. The hair follicles (HFs) were then removed by applying a drop of cyanoacrylate glue on the skin, followed by occlusion with adhesive tape. After 1 min, the tape was removed in a single motion. Finally, the remaining skin was cut into small fragments. We used the same technique to separate the layers of human skin; however, we excluded the step of obtaining the hair follicles, since this skin model is unsuitable for evaluating follicular drug delivery in vitro [21].

Each skin layer was individually placed in amber vials with 5 mL methanol for drug extraction and kept under moderate agitation (300 rpm) for 24 h. The extracts were filtered through a 0.45 µm membrane and analyzed through HPLC.

2.5. Chromatographic Conditions

A reverse-phase HPLC method (LC-20AD, Shimadzu, Kyoto, Japan) was employed using a C$_{18}$ column measuring 150 mm × 4.5 mm, 5 µm (Discovery®, Supelco, Germany) as the stationary phase and acetonitrile and 0.01 mol/L phosphoric acid at pH 3.5 as the mobile phase, with a flow rate fixed at 1.0 mL/min. Different mobile phase compositions (acetonitrile/phosphoric acid at 40:60 or 35:65 *v/v*), oven temperatures (30 or 35 °C), and injection volumes of the samples (10 or 20 µL) were tested to obtain optimal separation and peak resolution. IBR was detected at 259 nm [18]. The Shimadzu LC software performed data acquisition, analysis, and reporting.

2.6. Validation

The selected method was validated according to ICH guideline Q2 (R1) [22], considering selectivity, linearity, precision, accuracy, detection and quantification limits (LOD and LOQ), and robustness, considering the presence of skin interferents.

2.6.1. Selectivity

The HPLC method's ability to quantify and distinguish IBR from possible interferents was evaluated by testing solutions containing 7.5 µg/mL of IBR in the absence and presence of skin contaminants extracted from each skin layer using the tape-stripping technique described above. This assay was repeated six independent times for each matrix, and the drug's peak areas and retention time were analyzed.

2.6.2. Linearity

Three calibration curves were prepared using three different stock solutions of IBR to evaluate the linearity. Each aliquot was diluted in methanol, resulting in a calibration curve ranging from 0.2 to 15.0 µg/mL. The IBR concentration was plotted against the instrumental response (peak area), and the linearity was determined using the least-squares linear regression method [15,17].

2.6.3. Limit of Detection and Limit of Quantification

The LOD and LOQ were determined based on the standard deviation and slope of the calibration curves using Equations (1) and (2):

$$LOD = (3.3 \times SD)/slope \tag{1}$$

$$LOQ = (10 \times SD)/slope \tag{2}$$

where SD is the standard deviation, and "slope" is the slope of the calibration curve [15,17].

2.6.4. Precision

Precision was evaluated in terms of repeatability and intermediate precision. Repeatability was assessed using three concentrations of IBR (1.0, 7.5, and 15.0 µg/mL) with three replicates of each concentration. Intermediate precision was evaluated by analyzing the samples on two different days, prepared by two different analysts, using the same concentrations of IBR. The results were expressed as their coefficient of variation (CV), calculated according to Equation (3):

$$CV\ (\%) = (\text{standard deviation})/\text{mean} \times 100 \tag{3}$$

2.6.5. Accuracy

The accuracy was evaluated as the recovery of a known concentration of IBR in each skin layer. First, the stratum corneum and hair follicle were separated from the remaining porcine skin, and the stratum corneum was separated from the remaining human skin, as described in Section 2.4. Next, the different layers of skin were placed in separate amber flasks, to which volumes of IBR equivalent to 5.0, 37.5, and 75.0 µg were placed. The solvent was evaporated, and 5 mL of methanol was added to each flask, resulting in concentrations of 1.0, 7.5, and 15.0 µg/mL of IBR. After 24 h under agitation (300 rpm), the samples were filtered through a 0.45 µm membrane for HPLC analysis. The percentage recovery of IBR was calculated by comparing the detected drug quantity from the different skin layers to the total drug added, as follows:

$$\text{recovery }(\%) = [(\text{measured concentration})/(\text{theoretical concentration})] \times 100 \tag{4}$$

2.6.6. Robustness

Three analytical parameters were chosen to assess robustness: variation in mobile phase composition (±2.0%), oven temperature (±2.0 °C), and mobile phase flow rate (±0.1 mL/min). All assays were conducted in triplicate using IBR samples at 7.5 µg/mL. System suitability parameters, including the resolution, theoretical plates, and symmetry factor, were evaluated, along with the peak area and retention time. Model validation was performed using an ANOVA test, with a significance level of 0.05.

2.7. Application of the Method in Experiments of Cutaneous Permeation

In vitro cutaneous permeation studies were conducted to confirm the analytical method's applicability [23]. Franz-type cells were assembled with porcine or human skin fragments between the donor and receptor compartments, with the stratum corneum facing up. The receptor compartment was filled with 15 mL of a 30% ethanol solution in phosphate buffer (0.01 mol/L, pH 7.4) to ensure sink condition and kept under constant

agitation (500 rpm). Then, 500 μL of an ethanolic solution containing 1 mg/mL of IBR was placed onto the skin surface, and the experiment was carried out for 24 h at 32 °C.

At the end of the experiment, the skin fragments were removed from the diffusion cells, cleansed with distilled water, and dried, and the skin layers were separated by tape stripping, as previously described. Then, the different skin layers were placed in amber vials with 5 mL of methanol and, after 24 h of agitation (300 rpm) at room temperature and being filtered through a 0.45 μm membrane, the IBR was quantified using HPLC, following the validated analytical method. The results were expressed as the concentration of IBR recovered from the skin layers (μg/cm^2).

3. Results and Discussion

3.1. Establishment of Chromatographic Conditions

This study introduces the first validated analytical method for detecting and quantifying IBR using HPLC-UV in the presence of human or porcine skin contaminants.

A C$_{18}$ reversed-phase column was selected due to the low polarity of IBR (Log P = 3.97) [24], with an initial mobile phase composed of 40% acetonitrile and 60% phosphoric acid. In the first test, an aliquot of 20 μL of the IBR stock solution was injected into the column, and the oven was maintained at 30 °C (Figure 2A). Under these conditions, IBR eluted early (5.3 min), which did not ensure its total separation from the interfering agents from the skin. The acetonitrile proportion of the mobile phase was then changed to 35% to reduce the strength of the mobile phase, which increased the IBR elution to 8.7 min (Figure 2B). This variation in retention time was expected, as changes in the polarity of the mobile phase can either increase or decrease the interaction between the analyte and the stationary phase. In the case of IBR, its hydrophobic characteristics increase the retention time when using organic solvents with lower polarity, such as acetonitrile [25–27]. However, the separation had not yet proven efficient, as some overlapping peaks were still observed. Thus, a reduction in the injection volume of the sample (from 20 to 10 μL) was initially tested, which did not generate significant results (Figure 2C). Then, it was decided not to maintain such a reduction, given the absence of noticeable enhancements.
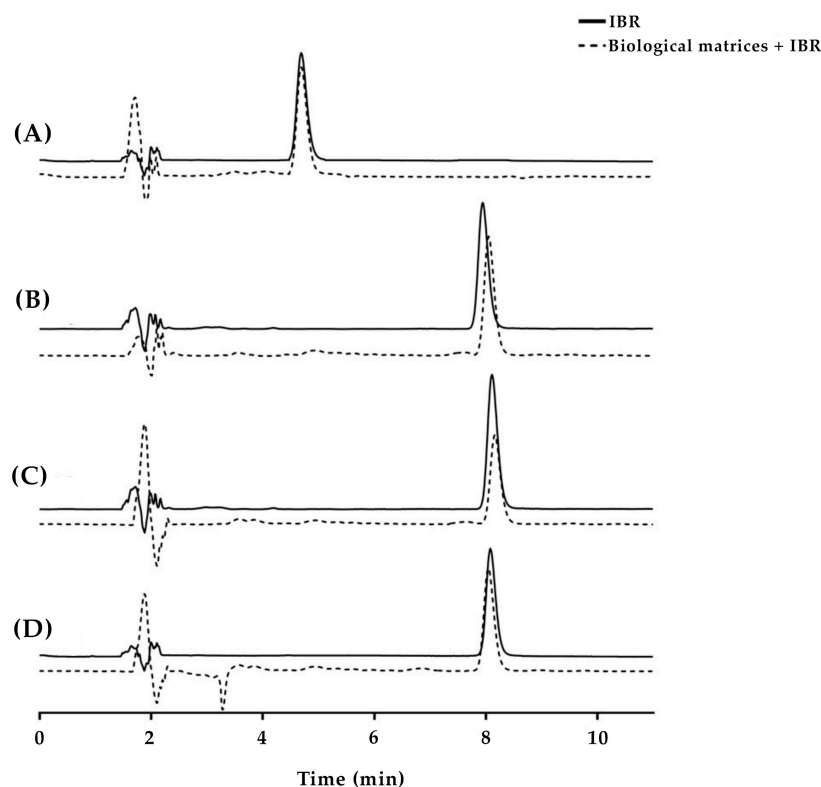

Figure 2. Representative chromatograms of IBR in the presence of skin contaminants obtained under various conditions, including different mobile phase compositions, oven temperatures, and sample

injection volumes. Chromatographic conditions: (**A**) mobile phase consisting of acetonitrile/0.01 mol/L phosphoric acid pH 3.5 (40:60), oven temperature set at 30 °C, and injection volume of 20 μL; (**B**) mobile phase consisting of acetonitrile/0.01 mol/L phosphoric acid pH 3.5 (35:65), oven temperature set at 30 °C, and injection volume of 20 μL; (**C**) mobile phase consisting of acetonitrile/0.01 mol/L phosphoric acid pH 3.5 (35:65), oven temperature set at 30 °C, and injection volume of 10 μL; (**D**) mobile phase consisting of acetonitrile/0.01 mol/L phosphoric acid pH 3.5 (35:65), oven temperature set at 35 °C, and injection volume of 20 μL.

Next, the oven temperature was increased by 5 °C to verify if a consequent reduction in the mobile phase viscosity could improve the IBR separation (Figure 2D). An increase in temperature is expected to enhance the fluidity of the mobile phase, which can result in better peak separation [27,28]. Indeed, this last measure efficiently led to a well-resolved IBR peak, which eluted at 8.9 min. The number of theoretical plates obtained was 8906, and the tailing factor was 1.2, which indicates that this was a suitable chromatographic method [27].

3.2. Validation

Samples with a known concentration of IBR (7.5 μg/mL) were supplemented with methanolic solutions derived from various layers of the skin to evaluate the method's selectivity. It is essential to emphasize the complexity of these biological matrices, as each skin layer possesses a distinct composition. For example, the extracts from the stratum corneum contain ceramides, fatty acids, and cholesterol, whereas the extract from the hair follicle includes contaminants from the sebaceous glands. Additionally, the remaining skin exhibits diverse contaminants from the extracellular matrix [17]. Consequently, a versatile method that can reliably detect IBR in different biological matrices is indispensable for permeation experiments.

The samples were then analyzed by comparing the drug peak area and retention time in the absence and presence of the contaminants and eliminating the possibility that the biological matrices exerted some effect of increasing or suppressing the peak area or altering the elution time of the drug. The chromatograms demonstrated the method's suitability, i.e., no vital difference in the chromatographic performance was noted in the presence of each skin contaminant (Figure 3).

Moreover, Figure 4A shows that skin contaminants did not significantly alter the IBR peak area ($p = 0.2730$, ANOVA). Figure 4B shows that the contaminants did not cause any marked difference in the drug retention time ($p = 0.1410$, ANOVA), which guarantees the selectivity of the analytical method.

The peak areas plotted against the concentration of IBR were found to be linear for the nine drug concentration points evaluated in the range of 0.2 to 15.0 μg/mL, showing a relevant area/concentration proportionality [24]. The linear regression calculation resulted in the following equation: $y = 50579x - 347.13$, with a linear coefficient of 0.9996, higher than the recommended minimum value. The high slope value of the curve (50,579) indicates that the method is probably sensitive [15,28,29].

In fact, the LOQ was calculated to be 0.021 μg/mL, and the LOD was 0.007 μg/mL. Notably, these limits were lower than the lowest point on the analytical curve (0.2 μg/mL). These values are noteworthy as they reflect the desired sensitivity of the analytical method developed for quantifying IBR in cutaneous permeation studies. The method could accurately quantify the drug, even when low concentrations of IBR were distributed in the skin. This capability will be demonstrated further in this paper, highlighting the method's effectiveness in quantifying IBR in skin permeation assays.

Precision was assessed on two levels: repeatability and intermediate precision. These results were presented as coefficients of variation, and are summarized in Table 1. Notably, the coefficients of variation observed at different concentrations were all below 5%, which meets the criteria set by international validation agencies for method precision [16,29,30].
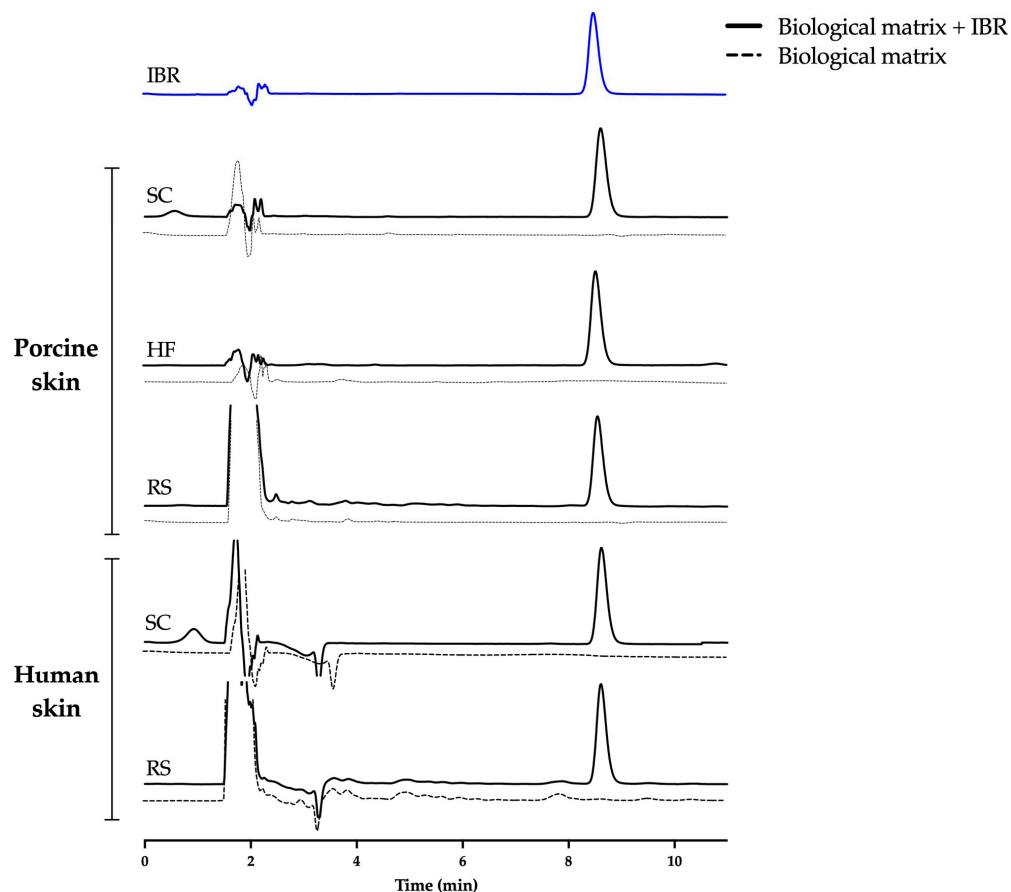
Figure 3. Representative chromatograms of IBR at 7.5 μg/mL in the presence of skin contaminants. SC = stratum corneum, HF = hair follicle, RS = remaining skin.
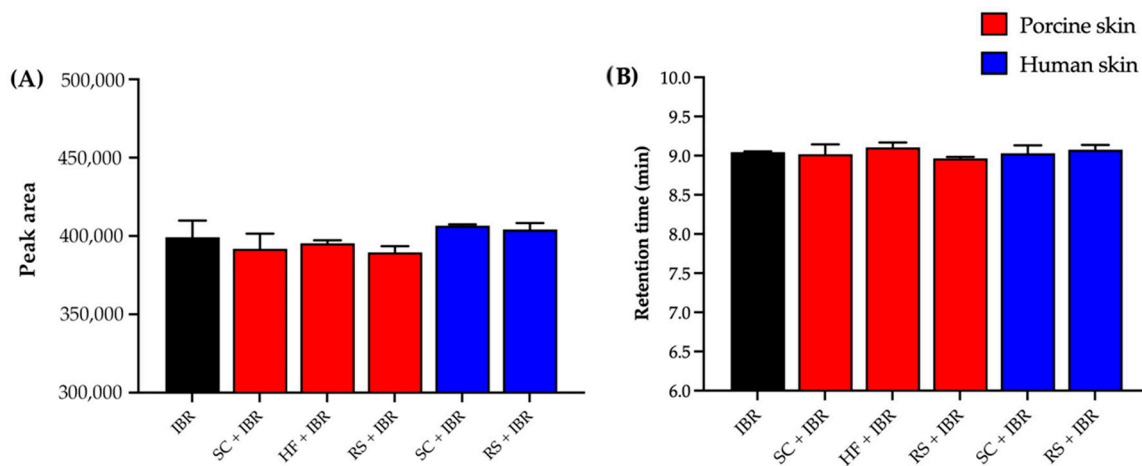

Figure 4. Results of selectivity in terms of (**A**) peak area and (**B**) retention time. SC = stratum corneum, HF = hair follicle, RS = remaining skin.

The accuracy of the analytical method was evaluated by measuring IBR recovery from different biological matrices, including the stratum corneum, hair follicle, and remaining skin. The recovery values for IBR ranged from 89.49 to 105.86% in porcine skin, depending on the layer evaluated, and 92.00 to 101.27% in human skin (Table 2). This recovery rate is within the limit established by international legislation [16,18,31].

Table 1. Results of precision test for the determination of IBR.

Day	Analyst	Theoretical Concentration (µg/mL)	Measured Concentration (µg/mL)	CV [1] (%)
1	A	1	1.01 ± 0.01	0.06
		7.5	7.79 ± 0.17	2.26
		15	15.47 ± 0.20	1.32
	B	1	0.96 ± 0.03	1.35
		7.5	7.27 ± 0.17	1.70
		15	14.86 ± 0.02	1.50
2	A	1	1.03 ± 0.01	2.59
		7.5	7.90 ± 0.12	2.21
		15	15.80 ± 0.22	0.12
	B	1	1.00 ± 0.03	3.06
		7.5	6.94 ± 0.10	1.48
		15	14.75 ± 0.22	1.53

[1] CV = coefficient of variation.

Table 2. Results of accuracy test for the determination of IBR.

Sample		Theoretical Concentration (µg/mL)	Measured Concentration (µg/mL)	CV [1] (%)	Accuracy (%)
Porcine skin	Stratum corneum	1.00	1.03 ± 0.01	1.05	102.67
		7.50	7.49 ± 0.15	2.16	99.91
		15.00	15.34 ± 0.08	0.52	102.27
	Hair follicle	1.00	1.04 ± 0.04	3.89	104.07
		7.50	7.88 ± 0.08	1.13	105.08
		15.00	15.88 ± 0.19	1.26	105.86
	Remaining skin	1.00	1.00 ± 0.03	2.79	104.32
		7.50	7.03 ± 0.09	1.34	93.72
		15.00	13.42 ± 0.89	6.64	89.49
Human skin	Stratum corneum	1.00	1.01 ± 0.01	0.89	101.27
		7.50	7.65 ± 0.01	0.10	102.00
		15.00	14.94 ± 0.03	0.19	99.63
	Remaining skin	1.00	1.00 ± 0.01	1.31	100.04
		7.50	6.90 ± 0.01	0.18	92.00
		15.00	13.82 ± 0.01	0.09	92.12

[1] CV = coefficient of variation.

Such results demonstrate the used analytical method's ability to accurately determine IBR in these two skin models when used in skin permeation experiments to evaluate topical formulations.

The method's robustness was assessed based on the responses obtained from challenging parameters, which included the oven temperature, mobile phase proportion, and mobile phase flow rate (Table 3). Variations in the mobile phase composition influenced the retention time of IBR. As expected, an increase in acetonitrile content decreased IBR's retention time, consistent with its nonpolar nature [32]. Changes in the flow rate also affected retention time, with higher rates resulting in shorter retention times for IBR. Moreover, adjustments to the oven temperature, flow rate, and mobile phase composition affected the tailing factor. Decreasing the temperature or flow rate tended to increase the tailing factor, while reducing the acetonitrile proportion in the mobile phase had a negative impact. Modifications solely influenced peak resolution in the mobile phase composition. Despite impacting the number of theoretical plates, all parameters remained within acceptable limits [32].

Table 3. Results of robustness test.

Parameter	Tested Conditions	IBR Retention Time (min)	Tailing Factor	Peak Resolution	Theoretical Plates
Oven temperature (°C)	33	8.89 ± 0.01	1.18 ± 0.02	8.13 ± 0.2	8548 ± 27
	35	8.84 ± 0.02	1.17 ± 0.01	8.23 ± 0.2	7888 ± 27
	37	8.80 ± 0.01	1.17 ± 0.07	7.87 ± 0.1	8702 ± 155
Acetonitrile/0.01 mol/L phosphoric acid (pH 3.5) in the mobile phase	33:67	11.55 ± 0.02	1.13 ± 0.04	10.4 ± 0.4	9919 ± 5
	35:65	8.84 ± 0.02	1.17 ± 0.01	8.23 ± 0.2	7888 ± 27
	37:63	7.0 ± 0.01	1.17 ± 0.02	6.0 ± 0.2	7983 ± 397
Flow rate (mL/min)	0.9	9.78 ± 0.02	1.18 ± 0.02	9.51 ± 0.3	8889 ± 21
	1.0	8.84 ± 0.02	1.17 ± 0.01	8.23 ± 0.2	7888 ± 27
	1.1	8.07 ± 0.01	1.17 ± 0.03	7.98 ± 0.2	8364 ± 41

No significant difference was observed in the amount of drug detected between the stratum corneum and hair follicle of the porcine skin ($p = 0.3607$, ANOVA). However, a higher accumulation of IBR was found in the remaining skin ($p < 0.0001$, ANOVA), representing the deeper skin layers comprising viable epidermis and dermis. Regarding the human skin, there was also no significant difference in the amount of accumulated IBR between the stratum corneum and the remaining skin ($p = 0.8004$, *t*-test). The high partition coefficient of IBR (Log P = 3.97) favored IBR penetration through the lipidic stratum corneum, reaching the viable skin, thus yielding an expected outcome [33].

It is worth emphasizing that this method allowed for the detection of drug variations between each skin layer, even when only a reduced amount of IBR (approximately 1% to 5% of the applied drug) permeated the skin (Figure 5). The method successfully distinguished the amount of drug recovered from each skin layer and model. Additionally, it is important to highlight that our method differentiated the amounts of IBR in different skin layers, with a coefficient of variation within acceptable limits for analytical methods involving drug extraction from biological tissues [33].
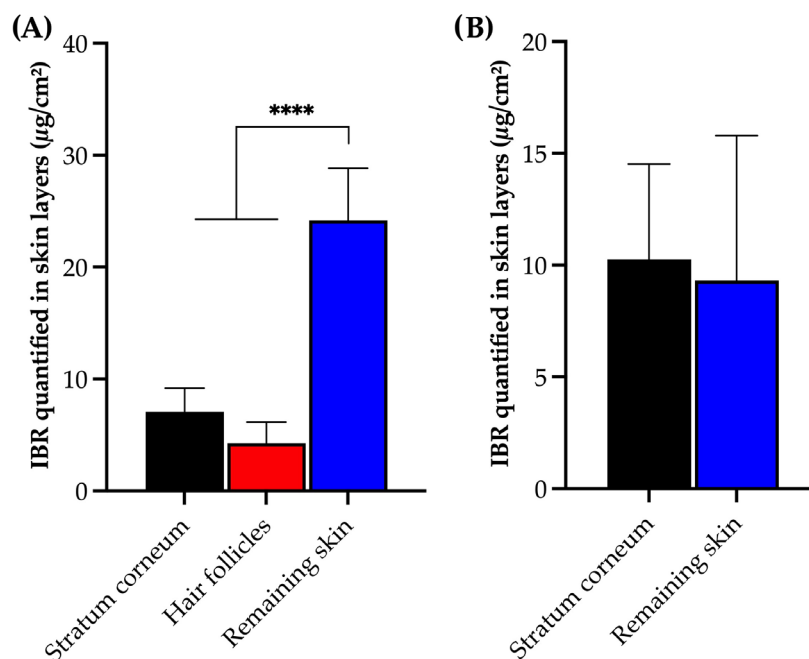

Figure 5. IBR recovered from (**A**) porcine and (**B**) human skin layers and quantified following the HPLC method after 12 h in vitro permeation experiments. Statistical analysis via ANOVA; **** $p < 0.001$.

Therefore, the results of this permeation study with human and porcine skin support the potential application of the developed analytical methodology to quantify IBR in

different skin layers accurately. This capability opens possibilities for developing new dermatological formulations for topical IBR treatment. Furthermore, given that in vitro permeation studies with human skin or its substitutes, such as porcine ear skin, utilizing Franz diffusion cells represent the gold standard for assessing the permeation behavior of specific drugs [20], our method demonstrated selectivity, linearity, sensitivity, and accuracy in detecting and quantifying IBR in the presence of contaminants from porcine and human skin, further solidifying its robustness. This observation aligns with similar findings from other validated methods for similar types of in vitro tests [17,23,32].

4. Conclusions

This validation was conducted according to ICH criteria. It showed that the analytical method proposed here is a selective, linear, and sensitive tool for detecting and quantifying IBR in the presence of skin interferents of different sources with precision and accuracy. Therefore, this method could support researchers in developing topical IBR formulations, particularly supporting studies involving in vitro permeation assays on both porcine and human skin.

References

1. Molina-Cerrillo, J.; Alonso-Gordoa, T.; Gajate, P.; Grande, E. Bruton's tyrosine kinase (BTK) as a promising target in solid tumors. *Cancer Treat. Rev.* **2017**, *58*, 41–50. [CrossRef]
2. Metzler, J.M.; Burla, L.; Fink, D.; Imesch, P. Ibrutinib in gynecological malignancies and breast cancer: A systematic review. *Int. J. Mol. Sci.* **2020**, *21*, 4154. [CrossRef]
3. Rangaraj, N.; Pailla, S.R.; Chowta, P.; Sampathi, S. Fabrication of ibrutinib nanosuspension by quality by design approach: Intended for enhanced oral bioavailability and diminished fast fed variability. *AAPS PharmSciTech* **2019**, *20*, 326. [CrossRef]
4. Varikuti, S.; Singh, B.; Volpedo, G.; Ahirwar, D.K.; Jha, B.K.; Saljoughian, N.; Viana, A.G.; Verma, C.; Hamza, O.; Halsey, G.; et al. Ibrutinib treatment inhibits breast cancer progression and metastasis by inducing conversion of myeloid-derived suppressor cells to dendritic cells. *Br. J. Cancer* **2020**, *122*, 1005–1013. [CrossRef]
5. Gomez-Rodriguez, J.; Kraus, Z.J.; Schwartzberg, P.L. Tec family kinases Itk and Rlk/Txk in T lymphocytes: Cross-regulation of cytokine production and T-cell fates: Cytokine regulation by Itk and Rlk/Txk. *FEBS J.* **2011**, *278*, 1980–1989. [CrossRef]
6. Luo, Q.-Y.; Zhou, S.-N.; Pan, W.-T.; Sun, J.; Yang, L.-Q.; Zhang, L.; Qiu, M.-Z.; Yang, D.-J. A multi-kinase inhibitor APG-2449 enhances the antitumor effect of ibrutinib in esophageal squamous cell carcinoma via EGFR/FAK pathway inhibition. *Biochem. Pharmacol.* **2021**, *183*, 114318. [CrossRef] [PubMed]
7. Wang, J.D.; Chen, X.Y.; Ji, K.W.; Tao, F. Targeting Btk with ibrutinib inhibit gastric carcinoma cells growth. *Am. J. Transl. Res.* **2016**, *15*, 3003–3012.
8. Rangaraj, N.; Pailla, S.R.; Shah, S.; Prajapati, S.; Sampathi, S. QbD aided development of ibrutinib-loaded nanostructured lipid carriers aimed for lymphatic targeting: Evaluation using chylomicron flow blocking approach. *Drug Deliv. Transl. Res.* **2020**, *10*, 1476–1494. [CrossRef] [PubMed]
9. Ashar, F.; Hani, U.; Osmani, R.A.M.; Kazim, S.M.; Selvamuthukumar, S. Preparation and optimization of ibrutinib-loaded nanoliposomes using response surface methodology. *Polymers* **2022**, *14*, 3886. [CrossRef] [PubMed]

10. Yang, Z.; Du, Y.; Lei, L.; Xia, X.; Wang, X.; Tong, F.; Li, Y.; Gao, H. Co-delivery of ibrutinib and hydroxychloroquine by albumin nanoparticles for enhanced chemotherapy of glioma. *Int. J. Pharm.* **2023**, *630*, 122436. [CrossRef] [PubMed]

11. Zhao, L.; Tang, B.; Tang, P.; Sun, Q.; Suo, Z.; Zhang, M.; Gan, N.; Yang, H.; Li, H. Chitosan/sulfobutylether-β-cyclodextrin nanoparticles for ibrutinib delivery: A potential nanoformulation of novel kinase inhibitor. *J. Pharm. Sci.* **2019**, *109*, 1136–1144. [CrossRef]

12. Ganatra, S.; Sharma, A.; Shah, S.; Chaudhry, G.M.; Martin, D.T.; Neilan, T.G.; Mahmood, S.S.; Barac, A.; Groarke, J.D.; Hayek, S.S.; et al. Ibrutinib-Associated Atrial Fibrillation. *JACC Clin. Electrophysiol.* **2018**, *4*, 1491–1500. [CrossRef] [PubMed]

13. Sibaud, V.; Beylot-Barry, M.; Protin, C.; Vigarios, E.; Recher, C.; Ysebaert, L. Dermatological Toxicities of Bruton's Tyrosine Kinase Inhibitors. *Am. J. Clin. Dermatol.* **2020**, *21*, 799–812. [CrossRef] [PubMed]

14. Csányi, E.; Bakonyi, M.; Kovács, A.; Budai-Szűcs, M.; Csóka, I.; Berkó, S. Development of topical nanocarriers for skin cancer treatment using quality by design approach. *Curr. Med. Chem.* **2019**, *26*, 6440–6458. [CrossRef] [PubMed]

15. Angelo, T.; Pires, F.Q.; Gelfuso, G.M.; da Silva, J.K.; Gratieri, T.; Cunha-Filho, M.S. Development and validation of a selective HPLC-UV method for thymol deter-mination in skin permeation experiments. *J. Chromatogr. B* **2016**, *1022*, 81–86. [CrossRef] [PubMed]

16. Demurtas, A.; Pescina, S.; Nicoli, S.; Santi, P.; de Araujo, D.R.; Padula, C. Validation of a HPLC-UV method for the quantification of budesonide in skin layers. *J. Chromatogr. B* **2020**, *1164*, 122512. [CrossRef] [PubMed]

17. Pereira, M.N.; Matos, B.N.; Gratieri, T.; Cunha-Filho, M.; Gelfuso, G.M. Development and validation of a simple chromatographic method for simul-taneous determination of clindamycin phosphate and rifampicin in skin permeation studies. *J. Pharm. Biomed. Anal.* **2018**, *159*, 331–340. [CrossRef] [PubMed]

18. Yasu, T.; Momo, K.; Yasui, H.; Kuroda, S. Simple determination of plasma ibrutinib concentration using high-performance liquid chromatography. *Biomed. Chromatogr.* **2019**, *33*, e4435. [CrossRef]

19. Jain, H.; Geetanjali, D.; Dalvi, H.; Bhat, A.; Godugu, C.; Srivastava, S. Liposome mediated topical delivery of Ibrutinib and Curcumin as a synergistic approach to combat imiquimod induced psoriasis. *J. Drug Deliv. Sci. Technol.* **2022**, *68*, 103103. [CrossRef]

20. Sim, Y.S.; Chong, Z.Y.; Azizi, J.; Goh, C.F. Development and validation of a gradient HPLC-UV method for mitragynine following in vitro skin permeation studies. *J. Chromatogr. B* **2022**, *1204*, 123316. [CrossRef]

21. Lademann, J.; Richter, H.; Meinke, M.; Sterry, W.; Patzelt, A. Which Skin Model Is the Most Appropriate for the Investigation of Topically Applied Substances into the Hair Follicles? *Skin Pharmacol. Physiol.* **2010**, *23*, 47–52. [CrossRef] [PubMed]

22. ICH. *Harmonised Tripartite Guideline—Validation of Analytical Procedures Text and Methodology—Q2 (R1)*; ICH: Geneva, Switzerland, 2005.

23. Cardoso, C.O.; Uwai, T.Y.; Gratieri, T.; Cunha-Filho, M.; Gelfuso, G. Chromatographic method for dacarbazine quantification in skin permeation experiments. *J. Pharm. Biomed. Anal.* **2023**, *234*, 115593. [CrossRef] [PubMed]

24. Simões, M.F.; Nogueira, B.A.; Tabanez, A.M.; Fausto, R.; Pinto, R.M.A.; Simões, S. Enhanced solid-state stability of amorphous ibrutinib formulations pre-pared by hot-melt extrusion. *Int. J. Pharm.* **2020**, *579*, 119156. [CrossRef] [PubMed]

25. Kazakevich, Y.V.; McNair, H.M. Low-energy interactions in high-performance liquid chromatography. *J. Chromatogr. A* **2000**, *872*, 49–59. [CrossRef] [PubMed]

26. Haun, J.; Teutenberg, T.; Schmidt, T.C. Influence of temperature on peak shape and solvent compatibility: Implications for two-dimensional liquid chromatography: Liquid chromatography. *J. Sep. Sci.* **2012**, *35*, 1723–1730. [CrossRef]

27. Walter, T.H.; Iraneta, P.; Capparella, M. Mechanism of retention loss when C8 and C18 HPLC columns are used with highly aqueous mobile phases. *J. Chromatogr. A* **2005**, *1075*, 177–183. [CrossRef] [PubMed]

28. Mcnair, H.; Polite, L.N. 17 Troubleshooting in high performance liquid chromatography. *Sep. Sci. Technol.* **2007**, *8*, 459–477.

29. ICH. *Q2 (R1) Validation of Analytical Procedures: Text and Methodology*; ICH: Geneva, Switzerland, 2006.

30. Duarah, S.; Sharma, M.; Wen, J. Rapid and simultaneous determination of dexamethasone and dexamethasone sodium phosphate using HPLC-UV: Application in microneedle-assisted skin permeation and deposition studies. *J. Chromatogr. B* **2021**, *1170*, 122609. [CrossRef]

31. Abraham, J. International Conference on Harmonisation of Technical Requirements for Registration of Pharmaceuticals for Human Use. In *Handbook of Transnational Economic Governance Regimes*; Tietje, C., Brouder, A., Eds.; Brill Publishers: Leiden, The Netherlands, 2010; pp. 1041–1053.

32. Quintão, W.S.; Ferreira-Nunes, R.; Gratieri, T.; Cunha-Filho, M.; Gelfuso, G.M. Validation of a simple chromatographic method for naringenin quantification in skin permeation experiments. *J. Chromatogr. B* **2022**, *1201–1202*, 123291. [CrossRef]

33. Tolentino, S.; Gratieri, T.; Cunha-Filho, M.; Gelfuso, G.M. Curcumin quantification in skin and mucosa: Optimization of extraction and chromatographic method validation. *J. Chromatogr. B Analyt. Technol. Biomed. Life Sci.* **2023**, *1217*, 123623. [CrossRef]